RSC Sustainability

ROYAL SOCIETY OF CHEMISTRY

PAPER

View Article Online
View Journal | View Issue

Cite this: *RSC Sustainability*, 2026, **4**, 466

A water-based synthetic route to the metal–organic framework UiO-66 starting from PET-derived terephthalate esters

Pietro Agola[a] and Marco Taddei *[ab]

The benchmark Zr-terephthalate MOF UiO-66 is typically prepared by solvothermal synthesis in *N*,*N*-dimethylformamide (DMF), one of the few solvents able to dissolve terephthalic acid. The use of DMF is one of the major drawbacks for the transfer of UiO-66 to large-scale applications, since DMF is an expensive and toxic organic solvent. In this work, we propose a water-based route to synthesise UiO-66 using either dimethyl terephthalate or bis(2-hydroxyethyl) terephthalate, which can be obtained from chemical recycling of waste polyethylene terephthalate, as a source of the linker. Hydrochloric acid and acetic acid were used as modulators during the synthesis to control the kinetics of ester hydrolysis and MOF crystallisation, aiming to avoid the collateral precipitation of terephthalic acid. A chemometric design of experiments was employed to optimise the reaction parameters, showing that 15 molar equivalents of hydrochloric acid enable hydrolysis without inhibiting crystallisation, while acetic acid controls which phase is obtained, favouring the desired face centred cubic topology at 15 molar equivalents. The optimised conditions afford UiO-66 with high crystallinity and porosity in just 2 hours at 90 °C. A crucial role in the process is played by the monoester, which is more soluble than both the diester and the diacid in the reaction environment and can be involved in the formation of secondary building units. We also developed a DMF-free workup protocol based on the use of ethanol/dimethylsulfoxide mixtures and water. A 50-fold scale up (500 mL) was demonstrated using a round bottom flask, producing UiO-66 with properties comparable to the product of the small-scale synthesis and with a space-time yield >200 kg m^{-3} d^{-1}.

Received 22nd June 2025
Accepted 25th November 2025

DOI: 10.1039/d5su00463b

rsc.li/rscsus

Sustainability spotlight

Metal–organic frameworks (MOFs) are a class of porous and crystalline materials that hold promise for a range of industrial applications, such as gas and vapour separation/storage, catalysis and sensors. For MOFs to be deployed in practical applications, it is necessary to make them commercially available at competitive costs, while ensuring the environmental sustainability of their production process. The UN sustainable development goal 12 (Ensure sustainable consumption and production patterns) dictates that the choice of metal, organic linker and solvents be made with care. Here, we focus on the benchmark Zr^{IV}-terephthalate MOF UiO-66, which combines a non-toxic metal with a widely available and biodegradable organic linker, but is usually synthesised in *N*,*N*-dimethylformamide (DMF), a flammable, toxic and teratogenic solvent whose use has been recently restricted by the European Union. We propose a water-based route to synthesise UiO-66 in just 2 hours at 90 °C using the terephthalate esters dimethyl terephthalate and bis(2-hydroxyethyl) terephthalate, which can be obtained from the methanolysis or glycolysis of waste PET, as a source of the linker. We also developed a workup protocol that replaces DMF with a mixture of the less toxic solvents dimethylsulfoxide and ethanol and demonstrated the scalability of the proposed synthetic approach.

Introduction

Almost three decades after the field had its inception, metal–organic frameworks (MOFs) are transitioning from academia to industry.[1,2] For MOFs to be deployed in practical applications, it is necessary to make them commercially available at competitive costs, focusing on MOFs that are not based on exotic, expensive or toxic raw materials and that can be synthesised on a large scale with sustainable routes.[3–5] Terephthalic acid (H_2BDC) is a precursor for the preparation of the ubiquitous polyethylene terephthalate (PET) polymer.[6] As such, it is a bulk chemical, largely available and cost-effective, and there is strong interest in MOFs based on terephthalate as the organic linker, such as MIL-53 (Al^{III}- or Cr^{III}-based),[7–9] MIL-88 (Fe^{III}-based),[10] MIL-125 (Ti^{IV}-based),[11] MIL-101 (Cr^{III}-based),[12] MOF-5 (Zn^{II}-based),[13] MIL-140 (Zr^{IV}-based)[14] and UiO-66 (Zr^{IV}-based).[15]

Among terephthalate-based MOFs, UiO-66, discovered in 2008, has rapidly become one of the most studied MOFs, owing to its high thermal, chemical and mechanical stability.[15–17] The

[a]*University of Pisa, Department of Chemistry and Industrial Chemistry, Via G. Moruzzi 13, 56124 Pisa, Italy. E-mail: marco.taddei@unipi.it*

[b]*Centro per l'Integrazione della Strumentazione scientifica dell'Università di Pisa (C.I.S.U.P.), University of Pisa, 56124 Pisa, Italy*

stability of UiO-66 is attributed to the strong Zr–carboxylate bonds and to the highly connected structure displaying a face centred cubic (fcu) topology based on twelve connected $Zr_6O_4(OH)_4(R–COO)_{12}$ secondary building units (SBUs). UiO-66 is typically prepared by solvothermal synthesis in *N*,*N*-dimethylformamide (DMF), a solvent also involved in the purification of the product.[15,18,19] This is necessary because of the limited solubility of the organic linker (H_2BDC) in both water and the most common organic solvents. The use of DMF is one of the major drawbacks for the transfer of UiO-66 to applications since DMF is flammable, toxic and teratogenic, besides being an expensive chemical.[20–22] The European Commission has recently proposed to restrict the industrial use and placement of DMF on the market because of its toxicity.[23] It is reasonable to suppose that, in the future, DMF will be subjected to more restrictions, and this would make DMF-based solvothermal synthesis unattractive from both an economic and an industrial perspective. To overcome the issues correlated with the use of DMF, it is necessary to develop alternative synthetic approaches.

Water is the ideal reaction medium because it is cheap, non-toxic, and available almost everywhere. Being very attractive from an economic and industrial perspective, several studies have focused on using water as solvent for the synthesis of UiO-66 based on functionalised analogues of H_2BDC, which display higher solubility than bare H_2BDC.[24–26] Reinsch *et al.* reported the water-based synthesis of UiO-66 starting from $Zr(SO_4)_2\cdot 4H_2O$ as the metal precursor and using $H_2BDC\text{-}NH_2$, $H_2BDC\text{-}(COOH)_2$ and $H_2BDC\text{-}F_4$ as the organic linkers. When $H_2BDC\text{-}NH_2$ and $H_2BDC\text{-}(COOH)_2$ were employed, sulfate was retained in the coordination sphere of Zr, yielding MOFs with an eight-connected body centred cubic (bcu) topology instead of the common twelve-connected fcu topology. Hu *et al.* reported the water-based synthesis of UiO-66 using different organic precursor, like H_2BDC, $H_2BDC\text{-}NH_2$, $H_2BDC\text{-}(OH)_2$, $H_2BDC\text{-}(COOH)_2$, $H_2BDC\text{-}(OCH_2CH_3)_2$, $H_2BDC\text{-}F_4$, and $H_2BDC\text{-}(COOH)_4$.[25] The reactions were conducted in a mixture of acetic acid and water at reflux for 24 h. A reassessment of the powder X-ray diffraction (PXRD) patterns suggests that only $H_2BDC\text{-}NH_2$, $H_2BDC\text{-}(OH)_2$ and $H_2BDC\text{-}F_4$ gave the desired UiO-66 with fcu topology and high crystallinity, while H_2BDC, $H_2BDC\text{-}(COOH)_2$, $H_2BDC\text{-}(OCH_2CH_3)_2$ and $H_2BDC\text{-}(COOH)_4$ gave low crystallinity products, whose patterns resemble those of hexagonal close packed (hcp) UiO-66, having a different chemical composition and crystal structure.[27,28] Dai *et al.* described the synthesis of crystalline UiO-66-COOH and UiO-66-NH_2 from the respective organic ligands $H_2BDC\text{-}COOH$ and $H_2BDC\text{-}NH_2$.[26] Reactions were conducted in water at room temperature for times ranging between 12 and 72 h, in the presence of a high content of formic acid as a crystallisation modulator and, in the case of UiO-66-NH_2, ethanol was used as a co-solvent.

Despite the possibility to use mild conditions and bypass the low solubility of H_2BDC, functionalised H_2BDC derivatives are less convenient compared to H_2BDC from an industrial standpoint because of their higher cost. Therefore, several efforts have been made to develop DMF-free syntheses of UiO-66. Morelli-Venturi *et al.* screened over 40 alternative solvents, usually considered to be green, identifying γ-valerolactone, propylene carbonate, Steposol, 1-(2-hydroxyehtyl)-1-pyrrolidone, *t*-amylmethyl ether and 1,3-propanediol as the most promising ones.[29] Dai *et al.* reported a room temperature ethanol-based synthesis of highly defective and nanocrystalline UiO-66, starting from acetate-capped $Zr_6O_4(OH)_4(CH_3–COO)_8(H_2O)_2Cl_3$ clusters and using comparatively small amounts of acetic acid and water to control the crystallisation process.[30] Very recently, Srikantamurthy *et al.* developed a water-based synthesis of UiO-66 that involves the *in situ* formation of $Zr_6O_4(OH)_4(CH_3–COO)_{12}$ clusters by combining $ZrOCl_2\cdot 8H_2O$ and acetic acid, followed by the addition of a solution of Na_2BDC and reaction at 65 °C for 24 h, obtaining UiO-66 with a yield of 89% and a moderate Brunauer–Emmett–Teller (BET) surface area of 760 $m^2\ g^{-1}$.[31] The authors of this work improved upon a concept previously published by Giri and co-workers, which afforded UiO-66 in low yield and with a low BET surface area.[32]

Commercially, the ideal reagent should contain the terephthalate moiety and be largely available and cheap. In principle, PET satisfies both these requirements. In the literature there are different examples of one-pot UiO-66 synthesis from PET in water, where the idea is to exploit the presence of water to hydrolyse PET and generate H_2BDC *in situ*. Conceptually, a synthesis in water that is also a way to upcycle PET itself is very interesting, but there are some issues related to the extreme reaction conditions. Waribam *et al.* reported the synthesis of UiO-66 from PET in water under microwave-assisted heating for 30 min at 200 °C in the presence of high concentrations of HCl (3 M, corresponding to 30 molar equivalents with respect to Zr) and acetic acid (4.35 M, corresponding to 43.5 molar equivalents with respect to Zr).[33] High temperature and high HCl content are necessary to overcome the chemical inertia of PET towards the hydrolysis reaction, while a high acetic acid content is necessary to slow down the crystallisation rate and produce crystalline samples at such high temperatures. There are other studies that focused on direct upcycling of PET through synthesis of UiO-66 using different systems.[34,35] For example, Serre and co-workers reported a synthesis of UiO-66 from PET under solvothermal conditions, working with a mixture of acetone and formic acid at 160 °C, obtaining a highly crystalline hcp UiO-66. Despite the possibility of obtaining both the fcu and hcp UiO-66 phases from PET, synthetic processes such as the ones reported in these studies are not suitable for industrial applications and there is the need for optimising such extreme and prohibitive reaction conditions.

In this work, we propose a water-based route to synthesise UiO-66 through the reaction shown in Scheme 1. The terephthalate esters DMT and bis(2-hydroxyethyl) terephthalate (BHET), derived from the chemical recycling of PET *via* methanolysis and glycolysis, respectively,[36] were used as sources of H_2BDC, avoiding the use of DMF in both the synthesis and the purification stage.

Experimental section

Chemicals

DMT (≥99%), $ZrOCl_2\cdot 8H_2O$ (≥99.5%), $ZrCl_4$ (98%), AA (≥99.8%), HCl (37% in water), H_2BDC (≥97.5%), formic acid

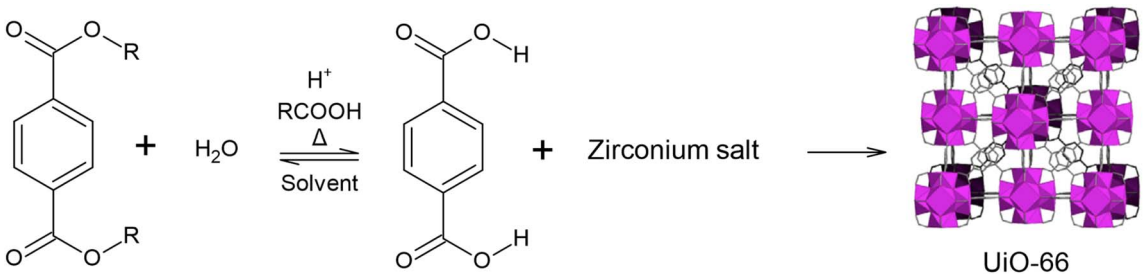

Scheme 1 Proposed one-pot synthetic route of UiO-66 starting from a terephthalate diester (R = $-CH_3$ or $-CH_2CH_2OH$).

(>98%), methanol (≥99.8%), monomethyl terephthalate (≥96.5), BHET (≥94.5%), DMF (≥99%), deuterium oxide D_2O (≥99%), triethylamine (TEA) (≥99%), and acetone (≥99.5%) were purchased from Sigma-Aldrich. Sodium hydroxide (NaOH) pellets, fumaric acid (≥99%), dimethyl sulfoxide (≥99.8%) and ethanol absolute anhydrous (≥99.9%) were purchased from Carlo Erba. All reagents were used as received.

Analytical procedures

Powder X-ray diffraction (PXRD). PXRD patterns were collected in the 5–30 °2θ range with a Rigaku MiniFlex 600 C diffractometer working in Bragg–Brentano geometry and equipped with a D/teX detector, using Cu Kα radiation (1.54056 Å). The X-ray tube was operated at a voltage of 40 kV and a current of 15 mA. Variable temperature PXRD (VT-PXRD) patterns were collected with an Anton Paar BTS-500 chamber. The calculated patterns for fcu and hcp UiO-66 were simulated from refcodes RUBTAK03 and KINGUM, respectively. The reo phase was instead generated by starting from refcode WIYFUJ, replacing Hf with Zr.

^{1}H nuclear magnetic resonance (NMR) analysis. Quantitative ^{1}H NMR analysis of the obtained solid was performed on a Jeol JNM-ECZ400S instrument equipped with a Royal Broadband probe. Chemical shifts are reported in parts per million (ppm). To be subjected to ^{1}H NMR analysis, samples needed to be digested. About 20 mg of sample was heated at 120 °C for three hours to remove traces of solvents and then digested for 24 hours in 1.0 mL of 1.0 M NaOH and 0.10 M fumaric acid (added as an internal standard) in D_2O. The NMR tubes were then loaded with the solution, which was filtered through cotton wool to avoid the presence of solid particles in dispersion. The spectra were collected with 4 scans and a recycle delay of 25 s.

Gas adsorption analysis. N_2 adsorption isotherms at 77 K were measured on a 3P micro 300 instrument (3P Instruments). The samples (about 70–130 mg) were kept overnight in an oven at 100 °C, and then activated for six hours under dynamic vacuum at 150 °C prior to analysis. BET surface areas were calculated in the 0.006–0.09 P/P_0 range, where all the criteria defined by Gomez-Gualdron *et al.*[37] were fulfilled.

Scanning electron microscopy (SEM). SEM micrographs were collected with a JEOL 7800F FEG SEM instrument with an acceleration voltage of 10 kV. The powders were deposited on carbon sticky tape on an aluminum support and sputtered with platinum with a Leica EM ACE600 sputterer, using an ultimate vacuum ≤2×10^{-6} mbar.

Thermogravimetric analysis (TGA). TGA was performed in air with a TA Instrument Thermo balance model Q5000IR using 2–4 mg of sample, with a heating rate of 5 °C min^{-1} up to 700 °C.

Small scale synthesis

1 mmol of $ZrOCl_2 \cdot 8H_2O$ (322 mg) was introduced in a vial (or in a Q-Tube® when the adopted temperature was higher than the normal boiling point of the solvent) and dissolved in an amount of distilled water or methanol sufficient to reach a total volume of 10 mL, followed by the addition of 1 mmol of the organic reagent (DMT, BHET, MMT or H_2BDC), and the chosen amount of AA and HCl. After that, a magnetic stir bar was added and the vial containing the mixture was put on a hot plate, stirred at 300 rpm and heated at a fixed temperature for different reaction times. The workup of the product was carried out in different ways, as detailed in the manuscript.

Large scale synthesis

400 mL of distilled water was added into a 1 L three necked round bottom flask and heated at a temperature of 90 °C. Heating was provided by a heating mantle and the temperature was monitored with a thermometer fitted in one of the necks. Once the desired temperature was reached, 0.05 mol (12.7 g) of ground BHET, 0.05 mol (16.1 g) of $ZrOCl_2 \cdot 8H_2O$, 40 mL of AA and 62.5 mL of 37% HCl were added to the reaction mixture. Agitation of the heterogeneous mixture was maintained by an overhead mechanical stirrer positioned in the central neck of the flask; furthermore, a condenser was put in the other lateral neck. The solid product was recovered by centrifugation at 5900 rpm and washed at a temperature of 70 °C under vigorous stirring two times with 250 mL of DMSO/EtOH (2 : 8 v/v) for 60 minutes and two times with 250 mL of water for 60 minutes, and once with 250 mL of EtOH. The solid was dried at 90 °C for two days in an oven. 8.64 g of desolvated product was recovered (Yield: 65%, based on Zr)

Synthesis of non defective_UiO-66 and defective_UiO-66

1 mmol of $ZrCl_4$ (233 mg) was introduced in a vial and dissolved in 20 mL (non defective_UiO-66) or 16.2 mL (defective_UiO-66) of DMF, followed by the addition of 1 mmol of H_2BDC (166 mg),

and, in the case of the synthesis of defective_UiO-66, 100 mmol of formic acid (4.6 g). After that, a magnetic stir bar was added and the vial containing the mixture was put on a hot plate, stirred at 300 rpm and heated at 120 °C for 16 h. The products were recovered by centrifugation and separated from the reaction mixture. Then, they were washed two times with 10 mL of DMF for 60 minutes, two times with 10 mL of water for 60 minutes and once with 10 mL of acetone for 60 minutes.

Results and discussion

Synthetic approach

As depicted in Scheme 1, our goal is to have a one-pot reaction, where H_2BDC is generated *in situ* by a controlled hydrolysis reaction of the respective diester. In this way, it is possible to bypass the low solubility of H_2BDC in the reaction medium, ensuring that it reacts with zirconium oxo-clusters as soon as it forms. Under optimal conditions, this avoids the accumulation of H_2BDC because it is removed from the equilibrium hydrolysis reaction and used to build the MOF as soon as it forms, thus favouring the hydrolysis reaction itself. A strong inorganic Brønsted acid, like HCl, is needed to catalyse the hydrolysis reaction on one hand, and on the other hand it acts a protonation modulator, slowing down crystallisation by maintaining the organic ligand in its protonated form.[18] To further control the crystallisation process, acetic acid (AA) was chosen as a coordination modulator, able to compete with H_2BDC for coordination to the metal, because it is commercially available and a green substance.[38,39] Furthermore, AA displays a high affinity towards both DMT and BHET, so it could also play a role in regulating their solubility in the reaction medium. $ZrOCl_2 \cdot 8H_2O$ was chosen as the Zr^{IV} source because of its lower hygroscopic character compared to the other commonly used precursor, *i.e.*, $ZrCl_4$.

The outcome of the syntheses was evaluated both qualitatively and quantitatively. From a quality standpoint, phase identity, purity and crystallinity of the product were used as indicators. Here, the term "crystallinity" refers to crystallite size, which can be estimated based on the full width at half maximum (FWHM) of selected Bragg reflections in the PXRD pattern, provided that the same instrumental setup is employed for the analysis: the lower the FWHM, the larger the crystallite size.[19] To have a quantitative assessment of the syntheses, we used reaction mass efficiency (RME), defined as follows:

$$\mathrm{RME} = \frac{m_{\mathrm{MOF}}}{m_{\mathrm{Zr}} + m_{\mathrm{linker}}}$$

where m_{MOF} is the mass of the desolvated MOF obtained after workup, and m_{Zr} and m_{linker} are the masses of $ZrOCl_2 \cdot 8H_2O$ and the terephthalate precursor (H_2BDC, DMT or BHET) used for the reaction, respectively. The choice of RME as a metric was driven by the fact that more than one crystalline phase (fcu or hcp), each with a specific stoichiometry, could be obtained, and that defects could be present in the framework, creating further uncertainty about the actual chemical composition of the product. RME, being a purely mass-based parameter, is agnostic to the chemical composition, but allows normalisation of the reaction yield, making it a better indicator than the bare mass of the product for comparison purposes in the context of reaction optimisation.[19,40]

Preliminary synthetic screening

We performed a preliminary screening to identify the most important reaction parameters, starting from DMT as the precursor to H_2BDC. 1 mmol of both $ZrOCl_2 \cdot 8H_2O$ and DMT was employed, in a total volume of 10 mL. The stoichiometric ratio between metal and diester was kept fixed throughout the work to ensure the highest possible atom economy. Samples were purified with a DMF-free workup protocol based on washings with a 0.1 M solution of triethylamine (TEA) in methanol (MeOH), followed by further washing with MeOH and acetone (further details on the optimisation of the workup protocol are provided later in the manuscript). The parameters chosen for the screening were temperature (between 80 and 130 °C), time (between 5 and 24 h), and quantity of AA [between 10 and 20 molar equivalents (eq.)] and HCl (between 10 and 20 eq.) (Table S1 and Fig. S1–S4). Because of its low polarity, DMT is not soluble in water, so the syntheses were conducted in a heterogeneous mixture under vigorous stirring.

This preliminary screening suggested that a temperature of 90 °C is sufficient to afford an RME as high as 40% of the hcp phase [compared to a maximum theoretical value of 47%, if hcp UiO-66 of formula $Zr_{12}O_8(OH)_{14}(BDC)_9$ is assumed as the only product] in 24 h (sample P2, Table S1). Such a temperature is desirable, as it allows work at atmospheric pressure in common laboratory glassware. A hypothesis is that 90 °C is the optimal temperature where the kinetics of DMT hydrolysis and MOF crystallisation are best balanced. Moving away from this optimal temperature could mean favouring one reaction, while inhibiting the other, thus reducing the amount of product. Another important observation is that the amount of AA appears to regulate which crystalline phase is obtained: hcp is favored when 10 eq. of AA is used (samples P1, P2, P3 and P8, Table S1), whereas fcu (with additional reflections associated with defective domains with reo topology)[41] dominates when 20 eq. of AA is used (samples P5, P6, P7 and P9, Table S1). The amount of HCl seems to have an impact primarily on the RME: the larger the amount, the lower the RME. While larger amounts of HCl are likely to accelerate the kinetics of DMT hydrolysis, there is a negative effect on the crystallisation kinetics because the deprotonation of H_2BDC is inhibited.

Mechanistic hypothesis

Two possible pathways can lead to the formation of UiO-66 starting from DMT, as illustrated in Scheme 2. The first step of the reaction is the hydrolysis of the diester to the monoester through an equilibrium reaction. According to the literature, the monoester appears to be more soluble than the diester and BDC in most of the solvents.[42] Once the monoester is formed, two pathways can be hypothesised for the formation of the MOF. In pathway (1), the second hydrolysis is more kinetically favoured than the coordination of the carboxylic group of the monoester to Zr, and the monoester is completely hydrolysed to

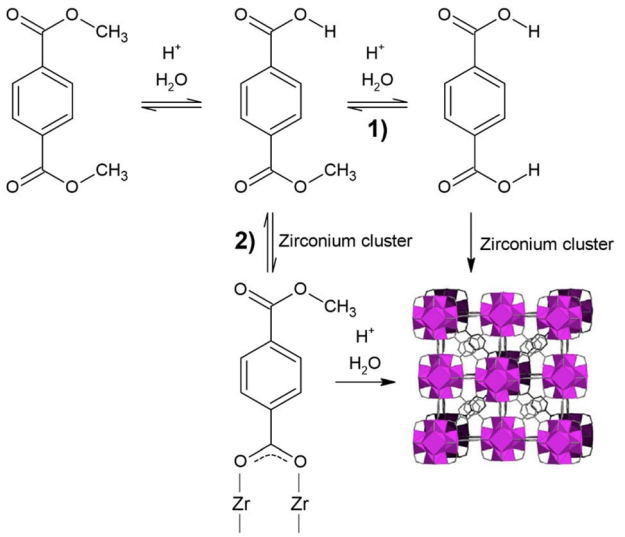

Scheme 2 Proposed pathways for the formation of UiO-66 starting from DMT.

H_2BDC, which then coordinates to Zr to produce an extended framework. In this mechanism, the diester simply acts as a reservoir of H_2BDC, which reacts as soon as it is formed. This allows, by optimising the reaction conditions, to avoid the accumulation and precipitation of H_2BDC from the reaction environment. In pathway (2), the coordination of the carboxylic group of the monoester with Zr is more kinetically favoured than the second hydrolysis and this coordination leads to the formation of soluble SBUs, followed by the second hydrolysis and expansion of the framework, with no formation of free H_2BDC.

To verify these hypotheses, H_2BDC was used as the organic precursor for the synthesis of UiO-66 in either water or MeOH as solvents. While no MOF was formed under any of the tested conditions in water (Table S2), the methanolic medium did afford fcu UiO-66, although with relatively low crystallinity (Table S3 and Fig. S5). These results suggest that the formation of the MOF proceeds either when starting from DMT under reaction conditions that allow hydrolysis, or when starting from H_2BDC and using reaction conditions that allow partial esterification. For further confirmation, a synthesis starting from the monoester, mono methyl terephthalate (MMT), was performed. The same reaction conditions used for DMT were employed to isolate the effect of the different organic precursor as a variable (Table S4 and Fig. S6), obtaining similar results.

Based on the evidence in our hands, it appears that the formation of the monoester from DMT is the key step for the formation of the MOF, and it is reasonable to hypothesise that it is the monoester, rather than H_2BDC itself, that coordinates to Zr in the first place, acting as a promoter for the formation of SBUs in solution. The growth of the MOF takes place following the hydrolysis of the second ester group. This hypothesis is consistent with some studies about the kinetics of both hydrolysis of DMT and esterification of H_2BDC, according to which the formation of monoester is more kinetically favoured compared to both the formation of diester (in the case of the esterification of H_2BDC) and the formation of H_2BDC (in the case of hydrolysis of DMT).[43,44]

Design of experiments

To optimise the synthesis of UiO-66, a chemometric design of experiments study was initially attempted starting from DMT. Because of problems correlated with the physical consistency of this diester (see the SI for more details), the reproducibility of the syntheses in terms of RME was limited, thus affecting the reliability of the results of the design of experiments. Therefore, we tested BHET as an alternative precursor. BHET has recently been demonstrated to be a suitable precursor for the solvent-free synthesis of UiO-66 performed by grinding BHET and the Zr^{IV} source together and heating the mixture at 130 °C for 12 h.[45] The suitability of BHET for our synthetic protocol was ascertained by performing syntheses under the same conditions previously used for DMT, obtaining analogous results (Table S5 and Fig. S7, S8). Unlike DMT, BHET has a physical consistency that allows it to be finely ground and was hence chosen as a reagent for the chemometric study.

A second-order model based on full factorial design, known as central composite design, was employed (see the ESI for details on the model). In these experiments, the temperature was fixed at 90 °C, the amounts of $ZrOCl_2 \cdot 8H_2O$ and BHET were fixed at 1 mmol, and the total volume was fixed at 10 mL. The independent variables to optimise were the amount of AA, the amount of HCl and the reaction time. AA and HCl were varied between 5 and 25 eq., with a central value of 15 eq., whereas time was varied between 5 and 26 h, with a central value of 16 h. The dependent variable to optimise was RME. The same workup protocol used in the preliminary experiments starting from DMT was used. Table 1 reports the full results of the 15 experiments performed and Table S6 reports the statistical significance of the calculated regression coefficients. Fig. 1 shows the response surface for RME depending on the amounts of AA and HCl at a fixed time of 16 hours.

In the surface displayed in Fig. 1, RME varies between 11 and 43%, and a non-monotonous trend is observed. It is evident that RME is inversely proportional to the concentration of AA. This agrees with the role of AA as a crystallisation inhibitor. Furthermore, it must be observed that, unlike the organic linker H_2BDC, AA is highly soluble in the reaction medium, which shifts the effective AA/H_2BDC ratio in solution towards AA. Regarding HCl, a quasi-parabolic trend is observed. First, it can be observed that its effect is less significant compared to that of AA. Second, it seems to have a positive effect on RME until a certain value is reached, and after that it tends to reduce it. This suggests that there is an optimal HCl content where both hydrolysis and reactive crystallisation are favoured, which agrees with the fact that HCl has a double effect on the overall process, favouring the hydrolysis on one hand and inhibiting the crystallisation on the other hand. No appreciable synergic effects are observed between AA and HCl. To maximise RME, it is therefore convenient to use an intermediate quantity of HCl, and theoretically a low AA content. However, it must be taken

Table 1 Results of the design of experiments study. Reaction conditions: total volume 10 mL, $ZrOCl_2 \cdot 8H_2O$: BHET 1 : 1, 90 °C. Workup protocol: 10 mL 0.1 M TEA in MeOH, 60 min × 2; 10 mL MeOH, 60 min × 2; 10 mL acetone, 60 min × 1

	Independent dimensionless variables			Independent variables			Y	
Sample	X_1	X_2	X_3	AA (eq)	HCl (eq)	t (h)	RME[a] (%)	Phase
P19	−1	1	−1	5	25	5	38	**fcu**
P20	1	−1	1	25	5	26	21	**fcu** + **hcp** + H_2BDC
P21	1	−1	−1	25	5	5	21	**fcu**
P22	1	1	1	25	25	26	16	H_2BDC + **fcu**
P23	1	1	−1	25	25	5	11	H_2BDC
P24	−1	−1	−1	5	5	5	36	**hcp**
P25	−1	1	1	5	25	26	25	**fcu** + H_2BDC
P26	−1	−1	1	5	5	26	34	**hcp**
P27	−1	0	0	5	15	16	42	**hcp**
P28	0	−1	0	15	5	16	34	**fcu**
P29	0	0	−1	15	15	5	43	**fcu**
P30	0	1	0	15	25	16	30	**fcu**
P31	0	0	1	15	15	26	43	**fcu**
P32	1	0	0	25	15	16	21	**fcu** + H_2BDC
P33	0	0	0	15	15	16	42	**fcu**

[a] Maximum RME obtainable starting from BHET and assuming an ideal defect free product with fcu topology of formula $Zr_6O_4(OH)_4(BDC)_6$ = 48%; maximum RME obtainable starting from BHET and assuming a product with hcp topology of formula $Zr_{12}O_8(OH)_{14}(BDC)_9$ = 42%.

into account that both AA and HCl also appear to regulate the selection of the crystalline phase obtained (Fig. 2, see Table S7 and Fig. S11–S15 for a univariate analysis of the effect of AA and Table S8 and Fig. S16–S20 for univariate analysis of the effect of HCl). Overall, the optimal conditions to obtain the highest RME of the hcp phase are 5 eq. AA and 15 eq. HCl (sample P27 in Table 1, RME = 42%), whereas the fcu phase is obtained with 15 eq. AA and 15 eq. HCl (samples P29, P31, and P33 in Table 1, RME = 42–43%) (Fig. 3).

Reaction time does not appear to have a strong influence on RME and a plateau is observed in the response surfaces obtained by keeping the amounts of either AA or HCl fixed (Fig. S9 and S10), suggesting that the reaction reaches complete conversion in less than 5 h. Time does not seem to have a significant influence on phase selection either, even though accumulation of H_2BDC appears to consistently take place at longer times (Table S9). To further investigate the effect of

Dimensionless variable	-1	0	1
AA (eq)	5	15	25
HCl (eq)	5	15	25

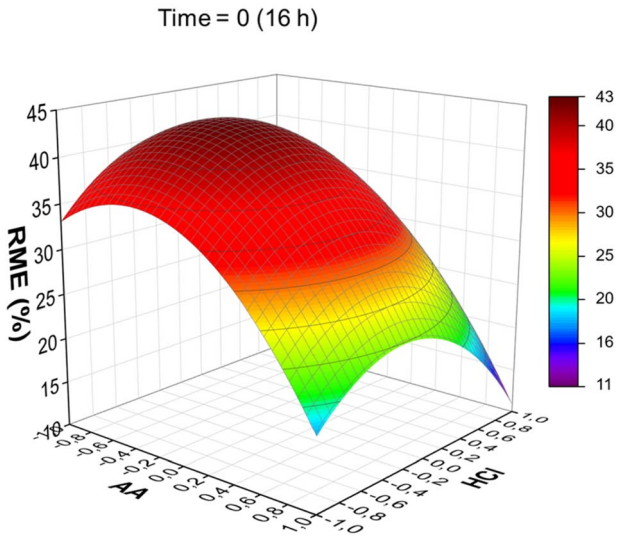

Fig. 1 Response surface for RME as a function of the amounts of AA and HCl at a fixed time of 16 hours.

HCl (eq) \ AA (eq)	5	15	25
5	hcp	fcu	fcu
15	hcp	fcu	fcu + H_2BDC
25	fcu	fcu	H_2BDC

Fig. 2 Summary of crystalline phases obtained with different combinations of AA and HCl.

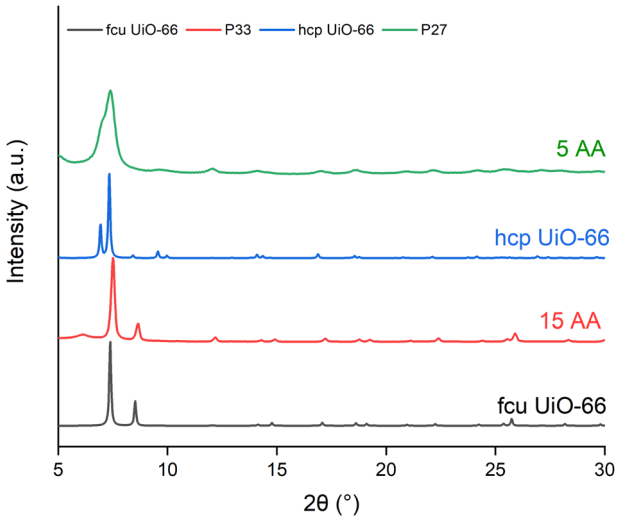

Fig. 3 PXRD patterns of P33 (red, 5 eq. AA, 15 eq. HCl, 16 h) and P27 (green, 15 eq. AA, 15 eq. HCl, 16 h). The calculated patterns for fcu UiO-66 (black, refcode RUBTAK03) and hcp UiO-66 (blue, refcode KINGUM) are also reported for comparison.

reaction time, the optimal reaction conditions involving 15 eq. AA and 15 eq. HCl for both product yield and quality were chosen (Table S10). To separate the contribution of the workup step from the RME, a workup protocol involving DMF washing was adopted for these experiments, so as to completely remove the unreacted H_2BDC. It was observed that most of the reaction takes place between one and two hours, and a plateau is reached after two hours. The PXRD pattern of the product obtained after two hours is practically identical to that of the product obtained after five hours (Fig. S21). It is noteworthy that the RME dropped from 43% in P29 (Table 1, corresponding to 90% yield based on Zr assuming defect-free fcu UiO-66) to 34% in P38 (Table S10, corresponding to 74% yield based on Zr assuming defect-free fcu UiO-66), both synthesised under the same conditions, suggesting that P29 might contain impurities that were not fully removed with the workup involving washing with 0.1 M TEA in MeOH used for the design of experiments study, a matter addressed in the next section.

Optimisation of the workup protocol

Having developed a DMF-free synthetic approach, we were also interested in the possibility of avoiding the use of DMF during the workup step. At this stage, the main difficulty consists in removing unreacted H_2BDC, derived from the hydrolysis of the diester, which has appreciable solubility only in DMF or in dimethylsulfoxide (DMSO). The other components, unreacted metal salt and diester, as well as AA and HCl, are easy to remove with polar solvents like water, alcohols or acetone. P38 (Table S10), washed with DMF (workup 1 in Table 2), was used as a reference sample where possible traces of unreacted H_2BDC can be excluded. Quantitative ^{1}H-NMR of P38 digested under alkaline conditions (Fig. S22) revealed that no organic species other than BDC^{2-} are present in the sample, suggesting that defects can only be compensated by hydroxide/water

Table 2 RME and wt% of the organic linker for samples obtained with the same synthetic conditions but different workup protocols

Sample	Workup protocol	RME (%)	BDC^{2-} [a] (wt%)
P38	1 [b]	34	50
P29	2 [c]	43	60
P39	3 [d]	35	46

[a] BDC^{2-} wt% in a defect-free MOF of ideal formula $Zr_6O_4(OH)_4(BDC)_6$ = 59%. [b] 10 mL DMF soaking × 2, 10 mL MeOH soaking × 2, 10 mL acetone. Soaking time: 90 minutes. [c] 10 mL 0.1 M TEA in MeOH × 2, 10 mL MeOH × 2, 10 mL acetone × 1. Soaking time: 60 minutes. [d] 5 mL DMSO/EtOH (2 : 8 v/v) × 2, 5 mL water x 2, 5 mL ethanol × 1. Filtered with Por 5.

couples.[46–48] The proposed chemical formula for P38 is $Zr_6O_4(OH)_4(BDC)_{4.68}(OH/H_2O)_{2.64}$, which suggests the presence of a large number of defects.

In an effort to develop a DMF-free workup protocol, we initially tried to exploit the acidic nature of H_2BDC by removing it using a base. Due to the susceptibility of the MOF to hydrolysis in the presence of hydroxide ions,[49,50] we chose to work with a 0.1 M solution of TEA in MeOH (workup 2 in Table 2). Although the PXRD pattern of P29, prepared under the same conditions as P38, did not display the presence of H_2BDC as a segregated phase, ^{1}H-NMR analysis (Fig. S23) revealed the presence of an excess of H_2BDC compared to the baseline represented by sample P38, suggesting that 3.75 H_2BDC molecules per Zr_6 cluster were trapped within the pores of the MOF. A new workup protocol was therefore developed, based on the use of DMSO, a high-boiling point ($T_{boiling}$ = 189 °C), polar aprotic solvent that displays high affinity for H_2BDC: 100 g of DMSO solubilises 19 g of H_2BDC at room temperature, *versus* 6.7 g of H_2BDC solubilised in 100 g of DMF.[51] In addition to this, DMSO is not toxic, since it displays a lower median lethal dose than ethanol (EtOH); this, together with its low volatility, makes it a relatively safe chemical compound. The main issue with its application as a solvent for workup is related to its high viscosity (1.99 mPa s at 25 °C),[52] which makes it difficult to remove from porous samples. Thus, we sought to exploit the high solubility of H_2BDC in DMSO, while blending it with EtOH (viscosity of 1.074 mPa s at 25 °C)[52] as a co-solvent. The optimal protocol for a synthesis performed on the 1 mmol scale involves filtering the solid and washing twice with 5 mL of a 20 : 80 DMSO/EtOH mixture, twice with 5 mL of water, and finally washing with 5 mL of EtOH (workup 3 in Table 2 and Fig. S24). Under these conditions, similar results, in terms of RME and wt% of BDC^{2-}, to those of workup 1 were obtained.

Characterisation

Having optimised both the synthesis and the workup protocol, P39 was further characterised by N_2 adsorption analysis at −196 °C, scanning electron microscopy (SEM), thermogravimetric analysis (TGA) and variable temperature PXRD (VT-PXRD). For the sake of comparison, two samples, named defective_UiO-66 and non defective_UiO-66, were synthesised

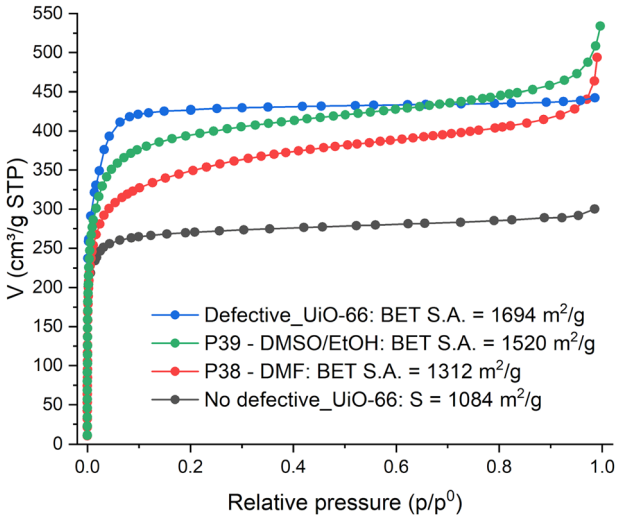

Fig. 4 N_2 adsorption isotherms (77 K) of P38 (red), P39 (green), non defective_UiO-66 (black) and defective_UiO-66 (blue).

following a classic literature procedure, involving DMF in both synthesis and workup.[53]

The N_2 isotherms of P38 and P39 exhibit a type I shape, which is consistent with the presence of micropores (Fig. 4). Non defective_UiO-66 displays the lowest surface area (1048 m^2 g^{-1}, Fig. S25), whereas defective_UiO-66 displays the highest surface area (1694 m^2 g^{-1}, Fig. S26) due to the presence of defects generated by formate (2.16 per cluster). Workup protocol 3 is very efficient in terms of removal of unreacted H_2BDC and residual DMSO, and this allows the pores to be completely freed, leading to a higher surface area (1520 m^2 g^{-1}, Fig. S27) than that obtained with workup protocol 1 (sample P38, 1312 m^2 g^{-1}, Fig. S28). Such high surface areas confirm that both P38 and P39 contain defects, as previously suggested by quantitative NMR analysis, and that P39 is in fact slightly more defective than P38.

SEM micrographs of P39 (Fig. S29) reveal aggregated crystallites with ill-defined morphology and size well below 1 μm, as opposed to the octahedral crystallites with sizes of hundreds of nm displayed by defective_UiO-66 (Fig. S30). The TG curve of P39 (Fig. 5a) displays a first mass loss of 33.9% in the 30–100 °C range, associated with desorption of water from the pores. Between 100 and 200 °C, another 3.8% loss of mass can be observed, which can be attributed to the removal of water coordinated to zirconium at defective sites. Between 200 and 450 °C, there is a gradual loss of mass, likely due to the progressive dehydroxylation of the zirconium clusters. Then, at 450 °C there is a final mass loss due to the thermal decomposition of the organic part of the framework that leads to the formation of ZrO_2 (the cumulated loss between 200 °C and 700 °C is 29.1%). By normalising the mass to the molar mass of the ZrO_2 residue (Fig. 5b), a comparison can be made with the expected mass of the desolvated and dehydroxylated MOF with formula $Zr_6O_{7.45}(BDC)_{4.55}$ (molar mass = 1411 g mol^{-1}) as derived from ^{1}H-NMR, showing good agreement. Using the formula $Zr_6O_4(OH)_4(BDC)_{4.55}(OH/H_2O)_{2.90}\cdot 2.1EtOH$, the yield

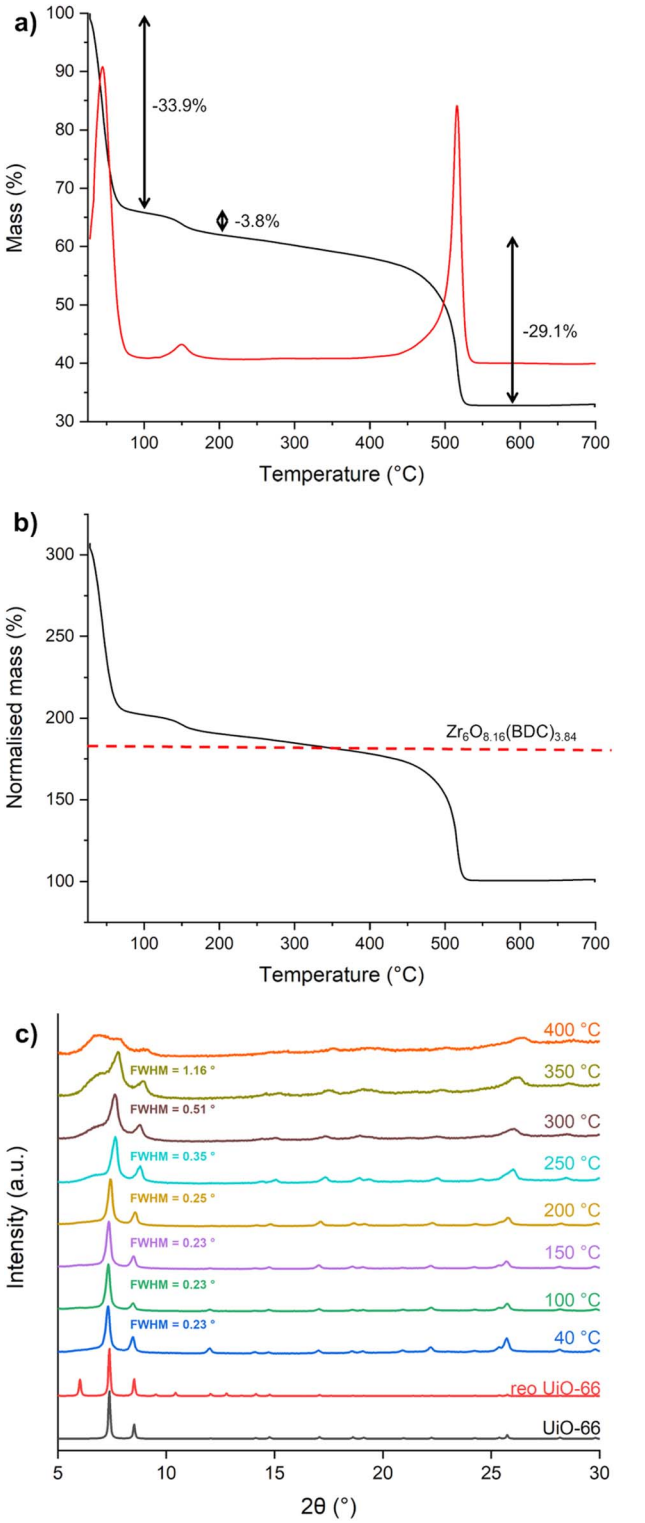

Fig. 5 TG curve of P39 (black) and the respective derivative curve (red) (a); TG curve of P39 with mass normalised to ZrO_2 and the expected normalised mass for the desolvated and dehydroxylated MOF (b); VT-PXRD patterns of P39 from 40 to 400 °C (c).

of P39 is 75%, based on Zr. VT-PXRD (Fig. 5c) suggests that the framework of P39 starts losing long range order above 200 °C and is fully collapsed at 400 °C. In comparison, defective_UiO-

66 fully retains its crystallinity until 300 °C, before collapsing above this temperature (Fig. S31). The different stabilities of the two defective MOFs can be ascribed to the larger amount of defects found in P39 and to different types of defect compensating species: water/hydroxide groups in P39 and formate groups in defective_UiO-66.

Synthesis scale up

A 50-fold synthesis scale-up (total volume of 500 mL) was performed under the same reaction conditions and with a similar workup protocol (same washing steps, but the solid was centrifuged instead of filtered because of the lack of a suitable filter for this scale) for sample P39 (sample P39_LS) using a round-bottom flask equipped with an overhead stirrer and a reflux condenser. 8.64 g of product were recovered from the large-scale synthesis, corresponding to an RME of 30% (slightly reduced from 35% in the small scale synthesis, most likely because of the slightly different workup procedure), to a yield of 65% based on Zr and to a space-time yield of 208 kg (m^{-3} d^{-1}) (calculated assuming 1 d = 24 h). The quality of P39_LS is comparable to that of P39, based on PXRD, 1H-NMR, N_2 adsorption analysis, TGA and VT-PXRD (Fig. S32–S36).

Conclusions

We developed a water-based method for the synthesis of UiO-66 from two commercially available terephthalate diesters, DMT and BHET, derived from the chemical depolymerisation of PET. The reaction was optimised with multivariate analysis, which allowed identification of optimal reaction conditions, in terms of the amount of acetic acid and hydrochloric acid and time, to maximise the MOF's yield and crystallinity, and to obtain either the hcp or fcu UiO-66 phases, depending on the amounts of acetic acid and hydrochloric acid in the reaction medium. The process uses mild reaction conditions (90 °C, 2 h) and does not involve DMF neither in the synthesis nor in the workup phase, making it sustainable from both the economic and the environmental standpoints. The process also proved to be promising when scaled 50-fold, giving a product having high crystallinity and purity, with comparable properties to those of the sample traditionally synthesised in DMF.

Conflicts of interest

There are no conflicts to declare.

Data availability

Data for this article, including raw PXRD, NMR, TGA and gas sorption data are available on Zenodo at https://doi.org/10.5281/zenodo.17475401.

Supplementary information (SI): additional tables, PXRD patterns, adsorption isotherms, BET fittings, NMR spectra, and SEM images. See DOI: https://doi.org/10.1039/d5su00463b.

Acknowledgements

The authors acknowledge the European Union's Horizon Europe research and innovation program for funding under grant agreement no. 101115488, within the EIC pathfinder project "DAM4CO_2". Eng. Randa Anis Ishak Nakhla (University of Pisa) is acknowledged for SEM micrographs. Dr Elena Pulidori and Maria Rita Carosi (University of Pisa) are acknowledged for TGA measurements. Dr Jan Demel and Dr Matous Kloda (Czech Academy of Sciences) are acknowledged for N_2 adsorption analysis.

References

1 A. M. Wright, M. T. Kapelewski, S. Marx, O. K. Farha and W. Morris, Transitioning Metal–Organic Frameworks from the Laboratory to Market through Applied Research, *Nat. Mater.*, 2025, **24**(2), 178–187, DOI: 10.1038/s41563-024-01947-4.

2 Z. Xie and J. Hou, Industrialising Metal–Organic Frameworks—Bridging Laboratory Innovation and Future Applications, *Ind. Eng. Chem. Res.*, 2025, **64**(16), 7941–7955, DOI: 10.1021/acs.iecr.5c00579.

3 M. I. Severino, E. Gkaniatsou, F. Nouar, M. L. Pinto and C. Serre, MOFs Industrialization: A Complete Assessment of Production Costs, *Faraday Discuss.*, 2021, **231**, 326–341, DOI: 10.1039/D1FD00018G.

4 K. Pobłocki, J. Drzeżdżon, B. Gawdzik and D. Jacewicz, Latest Trends in the Large-Scale Production of MOFs in Accordance with the Principles of Green Chemistry, *Green Chem.*, 2022, **24**(24), 9402–9427, DOI: 10.1039/D2GC03264C.

5 D. Chakraborty, A. Yurdusen, G. Mouchaham, F. Nouar and C. Serre, Large-Scale Production of Metal–Organic Frameworks, *Adv. Funct. Mater.*, 2024, **34**(43), 2309089, DOI: 10.1002/adfm.202309089.

6 R. A. F. Tomás, J. C. M. Bordado, J. F. P. Gomes and R. J. Sheehan, Terephthalic Acid, Dimethyl Terephthalate, and Isophthalic Acid, *Ullmann's Encyclopedia of Industrial Chemistry*, 2024, 1–17, DOI: 10.1002/14356007.a26_193.pub3.

7 C. Serre, F. Millange, C. Thouvenot, M. Noguès, G. Marsolier, D. Louër and G. Férey, Very Large Breathing Effect in the First Nanoporous Chromium(III)-Based Solids: MIL-53 or CrIII(OH)·{O2C−C6H4−CO2}·{HO2C−C6H4−CO2H} x·H2Oy, *J. Am. Chem. Soc.*, 2002, **124**(45), 13519–13526, DOI: 10.1021/ja0276974.

8 T. Loiseau, C. Serre, C. Huguenard, G. Fink, F. Taulelle, M. Henry, T. Bataille and G. Férey, A Rationale for the Large Breathing of the Porous Aluminum Terephthalate (MIL-53) Upon Hydration, *Chem. Eur. J.*, 2004, **10**(6), 1373–1382, DOI: 10.1002/chem.200305413.

9 F. Millange and R. I. Walton, MIL-53 and Its Isoreticular Analogues: A Review of the Chemistry and Structure of a Prototypical Flexible Metal-Organic Framework, *Isr. J. Chem.*, 2018, **58**(9–10), 1019–1035, DOI: 10.1002/ijch.201800084.

10 S. Surblé, C. Serre, C. Mellot-Draznieks, F. Millange and G. Férey, A New Isoreticular Class of Metal-Organic-Frameworks with the MIL-88 Topology, *Chem. Commun.*, 2006, (3), 284–286, DOI: 10.1039/B512169H.

11 M. Dan-Hardi, C. Serre, T. Frot, L. Rozes, G. Maurin, C. Sanchez and G. Férey, A New Photoactive Crystalline Highly Porous Titanium(IV) Dicarboxylate, *J. Am. Chem. Soc.*, 2009, **131**(31), 10857–10859, DOI: 10.1021/ja903726m.

12 G. Férey, C. Mellot-Draznieks, C. Serre, F. Millange, J. Dutour, S. Surblé and I. Margiolaki, A Chromium Terephthalate-Based Solid with Unusually Large Pore Volumes and Surface Area, *Science*, 2005, **309**(5743), 2040–2042, DOI: 10.1126/science.1116275.

13 H. Li, M. Eddaoudi, M. O'Keeffe and O. M. Yaghi, Design and Synthesis of an Exceptionally Stable and Highly Porous Metal-Organic Framework, *Nature*, 1999, **402**(6759), 276–279, DOI: 10.1038/46248.

14 V. Guillerm, F. Ragon, M. Dan-Hardi, T. Devic, M. Vishnuvarthan, B. Campo, A. Vimont, G. Clet, Q. Yang, G. Maurin, G. Férey, A. Vittadini, S. Gross and C. Serre, A Series of Isoreticular, Highly Stable, Porous Zirconium Oxide Based Metal–Organic Frameworks, *Angew. Chem., Int. Ed.*, 2012, **51**(37), 9267–9271, DOI: 10.1002/anie.201204806.

15 J. H. Cavka, S. Jakobsen, U. Olsbye, N. Guillou, C. Lamberti, S. Bordiga and K. P. Lillerud, A New Zirconium Inorganic Building Brick Forming Metal Organic Frameworks with Exceptional Stability, *J. Am. Chem. Soc.*, 2008, **130**(42), 13850–13851, DOI: 10.1021/ja8057953.

16 H. Wu, T. Yildirim and W. Zhou, Exceptional Mechanical Stability of Highly Porous Zirconium Metal–Organic Framework UiO-66 and Its Important Implications, *J. Phys. Chem. Lett.*, 2013, **4**(6), 925–930, DOI: 10.1021/jz4002345.

17 J. Winarta, B. Shan, S. M. Mcintyre, L. Ye, C. Wang, J. Liu and B. Mu, A Decade of UiO-66 Research: A Historic Review of Dynamic Structure, Synthesis Mechanisms, and Characterization Techniques of an Archetypal Metal–Organic Framework, *Cryst. Growth Des.*, 2020, **20**(2), 1347–1362, DOI: 10.1021/acs.cgd.9b00955.

18 M. J. Katz, Z. J. Brown, Y. J. Colón, P. W. Siu, K. A. Scheidt, R. Q. Snurr, J. T. Hupp and O. K. Farha, A Facile Synthesis of UiO-66, UiO-67 and Their Derivatives, *Chem. Commun.*, 2013, **49**(82), 9449–9451, DOI: 10.1039/C3CC46105J.

19 M. Taddei, P. V. Dau, S. M. Cohen, M. Ranocchiari, J. A. van Bokhoven, F. Costantino, S. Sabatini and R. Vivani, Efficient Microwave Assisted Synthesis of Metal–Organic Framework UiO-66: Optimization and Scale Up, *Dalton Trans.*, 2015, **44**(31), 14019–14026, DOI: 10.1039/C5DT01838B.

20 J. Hellwig, J. Merkle, H. J. Klimisch and R. Jäckh, Studies on the Prenatal Toxicity of N,N-Dimethylformamide in Mice, Rats and Rabbits, *Food Chem. Toxicol.*, 1991, **29**(3), 193–201, DOI: 10.1016/0278-6915(91)90037-8.

21 R. Stuart, Lessons Learned from a Short-Term Exposure to DMF, *ACS Chem. Health Saf.*, 2023, **30**(2), 44–48, DOI: 10.1021/acs.chas.2c00047.

22 S.-J. Hong, X.-N. Zhang, Z. Sun and T. Zeng, The Potential Health Risks of N,N-Dimethylformamide: An Updated Review, *J. Appl. Toxicol.*, 2024, **44**(11), 1637–1646, DOI: 10.1002/jat.4590.

23 Commission Regulation (EU), 2021/2030 of 19 November 2021 amending Annex XVII to Regulation (EC) No 1907/2006 of the European Parliament and of the Council concerning the Registration, Evaluation, Authorisation and Restriction of Chemicals (REACH) as regards N,N-dimethylformamide (Text with EEA relevance), https://eur-lex.europa.eu/legal-content/EN/TXT/?uri=uriserv:OJ.L_.2021.415.01.0016.01.ENG, (accessed 2025-06-18).

24 H. Reinsch, B. Bueken, F. Vermoortele, I. Stassen, A. Lieb, K.-P. Lillerud and D. De Vos, Green Synthesis of Zirconium-MOFs, *CrystEngComm.*, 2015, **17**(22), 4070–4074, DOI: 10.1039/C5CE00618J.

25 Z. Hu, Y. Peng, Z. Kang, Y. Qian and D. A. Zhao, Modulated Hydrothermal (MHT) Approach for the Facile Synthesis of UiO-66-Type MOFs, *Inorg. Chem.*, 2015, **54**(10), 4862–4868, DOI: 10.1021/acs.inorgchem.5b00435.

26 S. Dai, F. Nouar, S. Zhang, A. Tissot and C. Serre, One-Step Room-Temperature Synthesis of Metal(IV) Carboxylate Metal—Organic Frameworks, *Angew. Chem., Int. Ed.*, 2021, **60**(8), 4282–4288, DOI: 10.1002/anie.202014184.

27 M. Ermer, J. Mehler, M. Kriesten, Y. S. Avadhut, P. S. Schulz and M. Hartmann, Synthesis of the Novel MOF Hcp UiO-66 Employing Ionic Liquids as a Linker Precursor, *Dalton Trans.*, 2018, **47**(41), 14426–14430, DOI: 10.1039/C8DT02999G.

28 S. B. Peh, Y. Cheng, J. Zhang, Y. Wang, G. H. Chan, J. Wang and D. Zhao, Cluster Nuclearity Control and Modulated Hydrothermal Synthesis of Functionalized Zr12 Metal–Organic Frameworks, *Dalton Trans.*, 2019, **48**(21), 7069–7073, DOI: 10.1039/C8DT05060K.

29 D. Morelli Venturi, F. Campana, F. Marmottini, F. Costantino and L. Vaccaro, Extensive Screening of Green Solvents for Safe and Sustainable UiO-66 Synthesis, *ACS Sustainable Chem. Eng.*, 2020, **8**(46), 17154–17164, DOI: 10.1021/acssuschemeng.0c05587.

30 S. Dai, C. Simms, G. Patriarche, M. Daturi, A. Tissot, T. N. Parac-Vogt and C. Serre, Highly Defective Ultra-Small Tetravalent MOF Nanocrystals, *Nat. Commun.*, 2024, **15**(1), 3434, DOI: 10.1038/s41467-024-47426-x.

31 N. Hosadoddi Srikantamurthy, J. F. Olorunyomi, C. M. Doherty, P. C. Sherrell and X. Mulet, Aqueous Synthesis of UiO-66 Metal-Organic Frameworks With Enhanced Crystallinity and Surface Area, *Adv. Sustainable Syst.*, 2025, e00854, DOI: 10.1002/adsu.202500854.

32 L. Huelsenbeck, H. Luo, P. Verma, J. Dane, R. Ho, E. Beyer, H. Hall, G. M. Geise and G. Giri, Generalized Approach for Rapid Aqueous MOF Synthesis by Controlling Solution pH, *Cryst. Growth Des.*, 2020, **20**(10), 6787–6795, DOI: 10.1021/acs.cgd.0c00895.

33 P. Waribam, T. Rajeendre Katugampalage, P. Opaprakasit, C. Ratanatawanate, W. Chooaksorn, L. Pang Wang, C.-H. Liu and P. Sreearunothai, Upcycling Plastic Waste: Rapid Aqueous Depolymerization of PET and Simultaneous Growth of Highly Defective UiO-66 Metal-

Organic Framework with Enhanced CO2 Capture via One-Pot Synthesis, *Chem.–Eng. J.*, 2023, **473**, 145349, DOI: 10.1016/j.cej.2023.145349.

34 L. Zhou, S. Wang, Y. Chen and C. Serre, Direct Synthesis of Robust Hcp UiO-66(Zr) MOF Using Poly(Ethylene Terephthalate) Waste as Ligand Source, *Microporous Mesoporous Mater.*, 2019, **290**, 109674, DOI: 10.1016/j.micromeso.2019.109674.

35 M. C. Ribadeneyra, J. King, M. M. Titirici and P. Á. Szilágyi, A Facile and Sustainable One-Pot Approach to the Aqueous and Low-Temperature PET-to-UiO-66(Zr) Upcycling, *Chem. Commun.*, 2022, **58**(9), 1330–1333, DOI: 10.1039/D1CC06250F.

36 Z. Guo, J. Wu and J. Wang, Chemical Degradation and Recycling of Polyethylene Terephthalate (PET): A Review, *RSC Sustainability*, 2025, **3**(5), 2111–2133, DOI: 10.1039/D4SU00658E.

37 D. A. Gómez-Gualdrón, P. Z. Moghadam, J. T. Hupp, O. K. Farha and R. Q. Snurr, Application of Consistency Criteria To Calculate BET Areas of Micro- And Mesoporous Metal–Organic Frameworks, *J. Am. Chem. Soc.*, 2016, **138**(1), 215–224, DOI: 10.1021/jacs.5b10266.

38 M. Tobiszewski, J. Namieśnik and F. Pena-Pereira, Environmental Risk-Based Ranking of Solvents Using the Combination of a Multimedia Model and Multi-Criteria Decision Analysis, *Green Chem.*, 2017, **19**(4), 1034–1042, DOI: 10.1039/C6GC03424A.

39 A. Schaate, P. Roy, A. Godt, J. Lippke, F. Waltz, M. Wiebcke and P. Behrens, Modulated Synthesis of Zr-Based Metal–Organic Frameworks: From Nano to Single Crystals, *Chem.–Eur. J.*, 2011, **17**(24), 6643–6651, DOI: 10.1002/chem.201003211.

40 D. J. C. Constable, A. D. Curzons and V. L. Cunningham, Metrics to 'Green' Chemistry—Which Are the Best?, *Green Chem.*, 2002, **4**(6), 521–527, DOI: 10.1039/B206169B.

41 M. J. Cliffe, W. Wan, X. Zou, P. A. Chater, A. K. Kleppe, M. G. Tucker, H. Wilhelm, N. P. Funnell, F.-X. Coudert and A. L. Goodwin, Correlated Defect Nanoregions in a Metal–Organic Framework, *Nat. Commun.*, 2014, **5**(1), 4176, DOI: 10.1038/ncomms5176.

42 H. Zhang, Q. Xia, Y. Yang, F.-B. Zhang and G.-L. Zhang, Solubility of Dimethyl Terephthalate and Monomethyl Terephthalate in the Methanol Aqueous Solution and Its Application To Recycle Monomethyl Terephthalate from Crude Dimethyl Terephthalate, *Ind. Eng. Chem. Res.*, 2013, **52**(14), 5230–5234, DOI: 10.1021/ie400421e.

43 F. Campadelli and C. Nicora, A Study on the Esterification of Terephthalic Acid, *Eur. Polym. J.*, 1972, **8**(10), 1171–1178, DOI: 10.1016/0014-3057(72)90042-0.

44 M. Sim and M. Han, Hydrolysis of Dimethyl Terephthalate for the Production of Terephthalic Acid, *J. Chem. Eng. Jpn.*, 2006, **39**(3), 327–333, DOI: 10.1252/jcej.39.327.

45 P. A. Krisbiantoro, T.-J. Kuo, Y.-C. Chang, W. Liao, J.-P. Sun, C.-Y. Yang, Y. Kamiya, F.-K. Shieh, C.-C. Chen and K. C.-W. Wu, PET-Derived Bis(2-Hydroxyethyl) Terephthalate as a New Linker Source for Solvent-Free and Hydrothermal Synthesis of BDC-Based MOFs, *Mater. Today Nano*, 2024, **25**, 100459, DOI: 10.1016/j.mtnano.2024.100459.

46 M. Taddei, When Defects Turn into Virtues: The Curious Case of Zirconium-Based Metal-Organic Frameworks, *Coord. Chem. Rev.*, 2017, **343**, 1–24, DOI: 10.1016/j.ccr.2017.04.010.

47 M. J. Katz, R. C. Klet, S.-Y. Moon, J. E. Mondloch, J. T. Hupp and O. K. Farha, One Step Backward Is Two Steps Forward: Enhancing the Hydrolysis Rate of UiO-66 by Decreasing [OH–], *ACS Catal.*, 2015, **5**(8), 4637–4642, DOI: 10.1021/acscatal.5b00785.

48 J. M. Taylor, S. Dekura, R. Ikeda and H. Kitagawa, Defect Control To Enhance Proton Conductivity in a Metal–Organic Framework, *Chem. Mater.*, 2015, **27**(7), 2286–2289, DOI: 10.1021/acs.chemmater.5b00665.

49 D. Bůžek, J. Demel and K. Lang, Zirconium Metal–Organic Framework UiO-66: Stability in an Aqueous Environment and Its Relevance for Organophosphate Degradation, *Inorg. Chem.*, 2018, **57**(22), 14290–14297, DOI: 10.1021/acs.inorgchem.8b02360.

50 D. Bůžek, S. Adamec, K. Lang and J. Demel, Metal–Organic Frameworks vs. Buffers: Case Study of UiO-66 Stability, *Inorg. Chem. Front.*, 2021, **8**(3), 720–734, DOI: 10.1039/D0QI00973C.

51 C.-M. Park and R. J. Sheehan, Phthalic Acids and Other Benzenepolycarboxylic Acids, In *Kirk-Othmer Encyclopedia of Chemical Technology*, 2000, DOI: 10.1002/0471238961.1608200816011811.a01.

52 J. Rumble, *CRC Handbook of Chemistry and Physics*, CRC Press, 100th edn, Boca Raton, FL, 2019.

53 A. Koutsianos, E. Kazimierska, A. R. Barron, M. Taddei and E. Andreoli, A New Approach to Enhancing the CO2 Capture Performance of Defective UiO-66 via Post-Synthetic Defect Exchange, *Dalton Trans.*, 2019, **48**(10), 3349–3359, DOI: 10.1039/C9DT00154A.